

Detection of shorter-than-skin-depth acoustic pulses in a metal film via transient reflectivity

K. J. Manke,^{1, a)} A. A. Maznev,¹ C. Klieber,¹ V. Shalagatskyi,² V. V. Temnov,² D. Makarov,³ S.-H. Baek,⁴ C.-B. Eom,⁴ and K. A. Nelson¹

¹⁾*Department of Chemistry, Massachusetts Institute of Technology, Cambridge, Massachusetts, 02139, USA*

²⁾*Institut des Molécules et Matériaux du Mans, UMR CNRS 6283, Université du Maine, 72085 Le Mans cedex, France*

³⁾*Institute for Integrative Nanosciences, IFW Dresden, 01069 Dresden, Germany*

⁴⁾*Department of Materials Science and Engineering, University of Wisconsin-Madison, Madison, Wisconsin, 53706, USA*

(Dated: 13 July 2018)

The detection of ultrashort laser-generated acoustic pulses at a metal surface and the reconstruction of the acoustic strain profile are investigated. A 2 ps-long acoustic pulse generated in an SrRuO₃ layer propagates through an adjacent gold layer and is detected at its surface by a reflected probe pulse. We show that the intricate shape of the transient reflectivity waveform and the ability to resolve acoustic pulses shorter than the optical skin depth are controlled by a single parameter, which is determined by the ratio of the real and imaginary parts of the photoelastic constant of the material. We also demonstrate a Fourier transform-based algorithm that can be used to extract acoustic strain profiles from transient reflectivity measurements.

PACS numbers: 78.20.hc, 68.60.Bs, 68.55.

Keywords: Laser Ultrasonics, Thin Film Morphology

^{a)} Author to whom correspondence should be addressed. Electronic mail: kjmanke@mit.edu

Laser-based techniques for the generation and detection of short acoustic pulses have enabled ultrasonic measurements at the picosecond time scale and at frequencies up to and beyond 1 THz¹⁻⁴. The optical detection of ultrashort acoustic signals is often performed by measuring the transient reflectivity of thin metal films⁵. Because the probe light penetrates into the material over a finite distance given by the optical skin depth of the metal, the transient reflectivity signal does not directly reproduce the strain profile in the acoustic pulse^{5,6}. Recently Mante et al.⁷ demonstrated the detection of acoustic pulses significantly shorter than the optical absorption depth in semiconductor InP. The question remained whether shorter-than-skin-depth pulses could be measured with commonly used metal films, and, more importantly, whether the acoustic strain profile could be extracted from the intricate waveforms observed by Mante et al. Most recently, time-resolved plasmonic interferometry demonstrated that it is possible to measure acoustic pulses shorter than the skin depth of a surface plasmon in gold^{8,9}. It would be interesting to explore the capability of much simpler transient reflectivity measurements for the quantitative reconstruction of acoustic pulses.

In this paper, we investigate the transient reflectivity detection of ultrashort acoustic pulses in gold. We show that the reflectivity response of any strongly absorbing material to a shorter-than-skin-depth acoustic pulse can be decomposed into two terms. The first term contains a sharp step caused by the change in sign during the acoustic reflection at the free interface. This sharp step gives access to the acoustic pulse shape with sub-skin-depth spatial resolution, whereas the second slowly varying term is not sensitive to the structure of ultrashort acoustic waveforms. We identify the combination of photoelastic and optical constants that controls the ability to measure shorter-than-skin-depth pulses. Furthermore, we demonstrate a pulse reconstruction algorithm that can be used to recover the acoustic pulse profile from transient reflectivity measurements.

We use a gold/air interface for the detection of acoustic pulses generated in a very thin layer of single crystal SrRuO₃ (SRO) sandwiched between the gold layer and an SrTiO₃ (STO) substrate. The experimental geometry for the transient reflectivity measurements is pictured in Fig. 1(a). A single crystal SRO layer¹⁰ with a thickness of 12 nm was grown using 90 degree off-axis RF magnetron sputtering¹¹ at a rate of 1 nm/min. A polycrystalline gold film with a thickness of 200 nm and a primarily (111) texture, as determined by electron backscattering diffraction, was grown using magnetron sputtering. High-resolution scanning electron microscope (SEM) images of the gold film indicated that it had an average grain

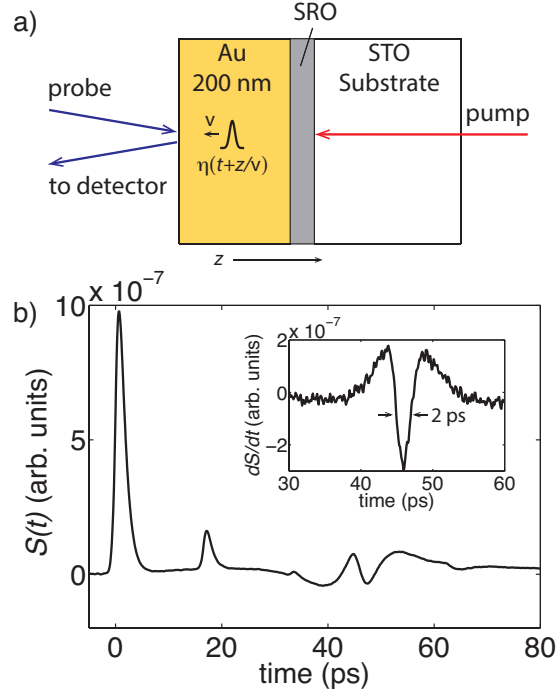


FIG. 1. (a) Schematic diagram of the sample structure and the experimental geometry; (b) the transient reflectivity signal $S(t)$ detected at the free surface of the gold layer shows the arrival of the acoustic pulse at a delay time of 46 ps. The inset shows the time derivative $dS(t)/dt$ of the reflectivity signal.

diameter of ~ 400 nm.

A Ti-sapphire oscillator with a regenerative amplifier was employed to generate laser pulses with a central wavelength of 786 nm and duration of 300 fs. The laser output was split into separate pump and probe beams and the probe beam was frequency-doubled to a wavelength of 393 nm. Illumination of the SRO transducer layer with the pump pulse through the 1 mm thick STO substrate launched an acoustic strain pulse through the gold layer, which was detected at the gold/air interface through the transient reflectivity of the variably delayed probe pulse.

The reflectivity signal $S(t)$ is depicted in Fig. 1(b). The sharp spike at zero pump-probe delay time arises from the optical generation of hot electrons at the gold/SRO interface followed by their ultrafast diffusion through the 150 nm thin gold layer on a sub-picosecond time scale¹². The barely visible slow rise in the background signal is due to the subsequent thermal diffusion^{9,13,14}. The small subsequent peaks at delay times of 18 ps and 35 ps are

caused by multiple roundtrips of the residual pump reflections within the 1 mm thick (STO) substrate. The optical signal at 46 ps marks the arrival of the acoustic strain pulse at the gold/air interface after propagating through the layer of (111) gold at the speed of sound $v = 3.45 \text{ nm/ps}^{15}$. It contains a fast 2-ps transient on top of a slowly varying component. The duration of the transient corresponds to the expected acoustic pulse duration generated in the SRO film given the speed of sound in SRO 6.31 m/s^{16} . In gold, this duration corresponds to a distance of 7 nm, significantly shorter than the skin depth of 16.5 nm^{17} .

The arrival of an acoustic strain pulse to within a skin depth of probe light results in a time-dependent strain profile $\eta_{33}(z, t)$ which induces a change in the complex reflection coefficient^{5,18}:

$$\frac{\delta\tilde{r}(t)}{\tilde{r}} = -i\frac{4\pi}{\lambda} \int_0^\infty \left(1 - \frac{2\tilde{n}}{1 - \tilde{n}^2} \frac{d\tilde{n}}{d\eta} \exp\left[i\frac{4\pi}{\lambda}\tilde{n}z\right]\right) \eta_{33}(z, t) dz, \quad (1)$$

with the complex refractive index $\tilde{n} = n + i\kappa$ and the photoelastic coefficient $d\tilde{n}/d\eta = dn/d\eta + id\kappa/d\eta$. Taking into account the reflection of the acoustic pulse $\eta(t)$ from the gold-air interface according to $\eta_{33}(z, t) = \eta(t + z/c_s) - \eta(t - z/c_s)$, we can rewrite this expression in the time domain

$$\frac{\delta\tilde{r}(t)}{\tilde{r}} = -i\frac{4\pi v}{\lambda} \int_{-\infty}^\infty [1 - (A + iB)e^{i4\pi\tilde{n}v|t' - t|/\lambda}] \text{sign}(t' - t)\eta(t') dt'. \quad (2)$$

where the complex dimensionless parameter $A + iB = 2\tilde{n}(d\tilde{n}/d\eta)/(1 - \tilde{n}^2)$ depends on both the photo-elastic coefficient $d\tilde{n}/d\eta$ and the index of refraction \tilde{n} .

The real part of this expression gives the reflectivity change $S(t)$ measured in our pump-probe experiment:

$$S(t) = \frac{\delta R(t)}{R} = 2\text{Re}\left[\frac{\delta\tilde{r}(t)}{\tilde{r}}\right] = \frac{8\pi v}{\lambda} \int_{-\infty}^\infty G(t' - t)\eta(t') dt', \quad (3)$$

with

$$G(t) = [A \sin(\omega_{\text{Br}}t) + B \cos(\omega_{\text{Br}}t) \text{sign}(t)]e^{-|t|/\tau_{\text{skin}}}. \quad (4)$$

Here we have introduced the Brillouin frequency¹⁹ $\omega_{\text{Br}} = 4\pi nv/\lambda = 2\pi \times 29 \text{ GHz}$ and the acoustic Time-of-flight $\tau_{\text{skin}} = \delta_{\text{skin}}/v = 4.8 \text{ ps}$ through the skin depth $\delta_{\text{skin}} = \lambda/(4\pi\kappa) = 16.5 \text{ nm}$ (the complex index of refraction of gold is $\tilde{n} = 1.67 + 1.94i^{17}$ at probe wavelength $\lambda = 393 \text{ nm}$).

The response function $G(t)$, which describes the reflectivity variation induced by an infinitely short acoustic pulse, represents the sum of two contributions. The first sine-term in Eq. (4) is a smooth function whose duration τ_{skin} is determined by the skin depth,

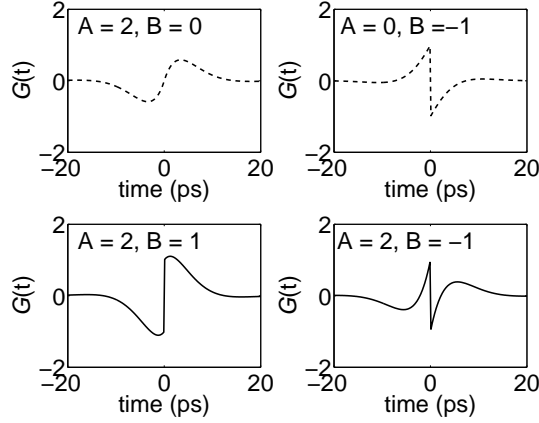


FIG. 2. The response function $G(t)$ (see Eq. 4) for different combinations of the coefficients A and B .

whereas the second cosine-term contains a sharp step. Fig. 2 shows both terms of the response function, as well as examples of a total response corresponding to $B/A = 1/2$ and $B/A = -1/2$. One can see that the shape of the transient reflectivity response is controlled by the ratio B/A :

$$\frac{B}{A} = \frac{\beta - \chi}{\beta\chi + 1}, \quad \chi = \left(\frac{dn}{d\eta} / \frac{d\kappa}{d\eta} \right), \quad \beta = \left(\frac{n}{\kappa} \right) \frac{n^2 + \kappa^2 - 1}{n^2 + \kappa^2 + 1}. \quad (5)$$

It is instructive to analyze the time derivative $dS(t)/dt$ of the transient reflectivity signal $S(t)$:

$$\frac{dS}{dt} = \frac{8\pi v}{\lambda} \left(2B\eta(t) + \int_{-\infty}^{\infty} F(t' - t)\eta(t')dt' \right), \quad (6)$$

with

$$F(t) = \left[\left(A\omega_{\text{Br}} - \frac{B}{\tau_{\text{skin}}} \right) \cos(\omega_{\text{Br}}t) - \left(B\omega_{\text{Br}} + \frac{A}{\tau_{\text{skin}}} \right) \sin(\omega_{\text{Br}}|t|) \right] e^{-|t|/\tau_{\text{skin}}}. \quad (7)$$

For a short acoustic pulse with duration $\tau_{\text{ac}} \ll \tau_{\text{skin}}$, the slowly varying integral term in Eq. (6) is proportional to τ_{ac} . Consequently, in the short-pulse limit the first term is dominant and the time derivative of the reflectivity response yields the acoustic strain profile. Indeed, in the signal derivative shown in the inset in Fig. 1(b), one can see a unipolar pulse of 2ps in duration. However, the pulse is not short enough for the slow component of the signal derivative to become negligible.

We see that in order to detect a short acoustic pulse, one needs a material and probe wavelength combination that yields a large value of B . One can see that B vanishes for a

weakly absorbing medium with vanishing κ , hence a strongly absorbing material is desired. On the other hand, B also vanishes in the limit $\kappa \gg n$. Thus a smaller skin depth is not necessarily preferred. Because detailed data on the wavelength dependence of the photoelastic constant $d\tilde{n}/d\eta$ are typically lacking, one has to resort to trial-and-error in search for the best material / wavelength combination.

We obtained an estimate of B/A for gold by fitting Eq. 6 to the time derivative of the reflectivity using a simulated strain pulse. Because the low acoustic impedance mismatch between STO and SRO suppresses the reflected wave ($Z_{\text{SRO}} = \rho_{\text{SRO}}v_{\text{SRO}} = 41 \times 10^6 \text{ kg m}^{-2} \text{ s}^{-1}$ and $Z_{\text{STO}} = \rho_{\text{STO}}v_{\text{STO}} = 40 \times 10^6 \text{ kg m}^{-2} \text{ s}^{-1}$)²⁰, we would expect the initial rectangular strain pulse to have a FWHM $\sim d_{\text{SRO}}/v_{\text{SRO}} = 1.90 \text{ ps}$. However, acoustic dispersion and the difference in the arrival time at the gold-air interface due to nanometer surface roughness cause the initial rectangular pulse shape to spread⁹. Therefore, we assumed a Gaussian pulse shape and allowed the width to vary to account for the overall acoustic broadening. The fit parameters were the ratio B/A and the FWHM of the Gaussian profile. To improve the efficacy of the fit, "echoes" caused by multiple reflections of the pump pulse inside the STO substrate were removed by subtracting time-delayed and scaled signal from the original data. The data pictured in Fig. 1 is an average over 25 scans; to test the repeatability of our fits, we divided the raw data files into five sets of five scans each and fit each set independently.

The results of fitting the full data set are shown in Fig. 3(a-c), along with the simulated strain pulse. The best results were obtained for $B/A = -0.59$ and FWHM = 2.54 ps. The statistical fitting error for B/A was 0.01; however, based on measurements of other samples we would suggest a more conservative error estimate of 0.03. Using our fit value for B/A , we obtained a ratio of $\chi=1.9$ at a wavelength of 393 nm. We expect a significant variation in the photoelastic constants of gold at visible wavelengths due to an interband transition in this region⁶. The known photo-elastic coefficients of other metals such as nickel and chromium have the same order-of-magnitude ratio $|\chi| \sim 1$ ¹⁸.

Quantitative acoustic measurements require a reliable algorithm for the reconstruction of an acoustic pulse profile $\eta(t)$. It was demonstrated recently that for ultrafast acousto-plasmonic measurements, the strain profile can be recovered from the plasmonic analog of Eq. (6) using an iterative numerical method⁹. However, in the case of reflectivity measurements, the coefficients of the sine and cosine terms in Eq. (7) are too large and the iterative solution of Eq. (6) diverges.

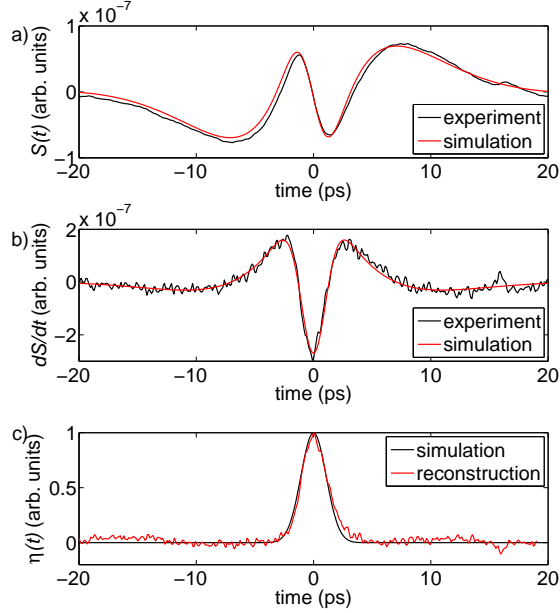


FIG. 3. (a) A comparison of the simulated reflectivity curve and the experimental data; (b) The time-derivative of the reflectivity data and the fit that was obtained for Eq. 6; and (c) A comparison of the simulated strain pulse and the reconstructed strain pulse.

A more general method for pulse reconstruction is demonstrated here. After taking the Fourier transform of Eq. 3 and applying the convolution theorem, the reconstructed strain in the Fourier domain is given by $\eta(\omega) = (\frac{\lambda}{4\pi v})S(\omega)/G(\omega)$ with

$$G(\omega) = \int_{-\infty}^{\infty} G(t)e^{-i\omega t} dt = -2i\omega \frac{(2\omega_{Br}/\tau_{skin})A + (\omega^2 - \omega_{Br}^2 + 1/\tau_{skin}^2)B}{(\omega^2 - \omega_{Br}^2 + 1/\tau_{skin}^2)^2 + (2\omega_{Br}/\tau_{skin})^2}. \quad (8)$$

Applying the inverse Fourier transform delivers the desired acoustic strain profile

$$\eta(t) = \frac{\lambda}{8\pi^2 v} \int_{-\infty}^{\infty} \frac{S(\omega)}{G(\omega)} e^{i\omega t} d\omega, \quad (9)$$

shown in Fig. 3(b). The reconstructed waveform matches the Gaussian pulse obtained by curve fitting fairly well. However, the reconstruction algorithm did not use any assumptions about the acoustic pulse shape and can be employed to recover arbitrary acoustic strain profiles.

The reconstructed waveform contains barely visible slow oscillations of the baseline which become more prominent when noisier data are analyzed. The spectral function $G(\omega)$ possesses three zeros, $\omega = 0$ and $\omega = \pm\omega_0 = \pm 2\pi \times 56$ GHz, resulting in singularities in

$\eta(\omega) = (\frac{\lambda}{4\pi v})S(\omega)/G(\omega)$ in the presence of noise with non-zero spectral components at these frequencies. The singularity at $\omega = 0$ is prevented by subtracting the slow background from the experimental signal $S(t)$ to guarantee $\int S(t)dt = 0$ ($S(\omega = 0) = 0$). The two other roots $\omega = \pm\omega_0$ result in a background modulation with a period of $2\pi/\omega_0 = 18$ ps. This modulation does not present a problem for the analysis of shorter-than-skin-depth acoustic pulses but may become a nuisance for longer waveforms containing significant frequency components at ω_0 . The existence of non-zero roots of $G(\omega)$ requires $\omega_{Br}^2 - 1/\tau_{skin}^2 > (A/B)(2\omega_{Br}/\tau_{skin})$ and can be avoided if different probe wavelengths and/or a different metal are used.

In conclusion, our results demonstrate that transient reflectivity can be used to detect shorter-than-skin depth acoustic pulses in common metals such as gold. The ability to resolve short acoustic pulses depends is not limited by the the skin depth of the material; rather, it is controlled by the parameter B/A that depends on the photoelastic constants and the the complex index of refraction at the detection wavelength. We have demonstrated a pulse reconstruction algorithm capable of recovering the acoustic pulse profile from transient reflectivity data which will advance quantitative ultrafast acoustic spectroscopy.

This work was supported in part by U. S. Department of Energy Grant DE-FG0200ER15087 and *Nouvelle équipe, nouvelle thématique de la Région Pays de La Loire*. The work of at University of Wisconsin-Madison was supported by the AFOSR through grant FA9550-12-1-0342 and Army Research Office through grant W911NF-10-1-0362. K.J.M. acknowledges support from a National Science Foundation Graduate Research Fellowship. D.M. acknowledges financial support from the European Research Council under the European Union's Seventh Framework Programme (FP7/2007-2013) / ERC grant agreement number 306277.

REFERENCES

- ¹H. T. Grahn, H. J. Maris, and J. Tauc, IEEE J. Quant. Electron. **25**, 2562 (1989).
- ²A. Yamamoto, M. Tomobumi, and Y. Masumoto, Phys. Rev. Lett. **73**, 740 (1994).
- ³C.-K. Sun, J.-C. Liang, and X.-Y. Yu, Phys. Rev. Lett. **84**, 179 (2000).
- ⁴A. A. Maznev, K. J. Manke, K.-H. Lin, K. A. Nelson, C.-K. Sun, and J.-I. Chyi, Ultrasonics **52**, 1 (2012).
- ⁵C. Thomsen, H. T. Grahn, H. J. Maris, and J. Tauc, Phys. Rev. B **34**, 4129 (1986).

- ⁶A. Devos and C. Lerouge, Phys. Rev. Lett. **86**, 2669 (2001).
- ⁷P.-A. Mante, A. Devos, and A. Le Louarn, Phys. Rev. B **81**, 113305 (2010).
- ⁸V. V. Temnov, Nature Photon. **6**, 728 (2012).
- ⁹V. V. Temnov, C. Klieber, K. A. Nelson, T. Thomay, V. Knittel, A. Leitenstorfer, D. Makarov, M. Albrecht, and R. Bratschitsch, Nature Comm. **4**, 1468 (2013).
- ¹⁰C. B. Eom, R. J. Cava, R. M. Fleming, J. M. Phillips, R. B. van Dover, J. H. Marshall, J. W. P. Hsu, J. J. Krajewski, and W. F. Peck Jr., Science **258**, 1766 (1992).
- ¹¹C. B. Eom, J. Z. Sun, K. Yamamoto, A. F. Marshall, K. E. Luther, T. H. Geballe, and S. S. Laderman, Appl. Phys. Lett **55**, 595 (1989).
- ¹²S. D. Brorson, J. G. Fujimoto, and E. P. Ippen, Phys. Rev. Lett. **59**, 1962 (1987).
- ¹³G. Tas and H. J. Maris, Phys. Rev. B **49**, 15046 (1994).
- ¹⁴M. Lejman, V. Shalagatskyi, O. Kovalenko, T. Pezeril, V. V. Temnov, and P. Ruello, arXiv:1304.5391 (2013).
- ¹⁵O. Anderson, in *Physical Acoustics, IIIB*, edited by W. Mason (Academic Press, New York, 1965) pp. 43–95.
- ¹⁶S. Yamanaka, T. Maekawa, H. Muta, T. Matsuda, S.-i. Kobayashi, and K. Kurosaki, J. Solid State Chem. **98**, 3484 (2004).
- ¹⁷D. W. Lynch and W. R. Hunter, in *Handbook of optical constants of solids*, edited by E. Palik (Elsevier, 1998) pp. 275–316.
- ¹⁸T. Saito, O. Matsuda, and O. B. Wright, Phys. Rev. B **67**, 205421 (2003).
- ¹⁹H.-N. Lin, R. J. Stoner, H. J. Maris, and J. Tauc, J. Appl. Phys. **69**, 3816 (1991).
- ²⁰R. O. Bell and G. Rupprecht, Phys. Rev. **129**, 90 (1963).